

Special Issue of the 6th International Congress & Exhibition (APMAS2016), Maslak, Istanbul, Turkey, June 1–3, 2016

An Investigation of Microstructure and Mechanical Properties of Sn–9Zn– x Cr Alloys Produced by Investment Casting Method

B. YAVUZER* AND D. OZYUREK

Karabuk University, Technology Faculty, Manufacturing Eng., 78100 Karabuk, Turkey

In this study, the microstructure and mechanical properties were investigated of different amount Cr (0.1%, 0.5%, 0.9%) added Sn–9Zn eutectic alloys and Weibull statistical analyses were evaluated using ultimate tensile strength. Pure elements (Sn, Zn, Cr) were used for production of alloys and pre-alloying was done and waited in the electrical resistance furnace at 450 °C for 1 h to homogenized and poured as ingot in plaster moulds. Then pre-alloyed Sn–9Zn– x Cr ingots were melted and poured at 300 °C in ceramic moulds prepared investment casting method. As a result of the study, the highest hardness and ultimate tensile strength values were measured in the Sn–9Zn alloy with 0.1% Cr. It was determined that while ultimate tensile strength was decreased, percentage of elongation was increased by increase of Cr amount. According to the Weibull statistical analyses results, the highest Weibull module was calculated by Sn–9Zn–0.1Cr alloy ultimate tensile strength values.

DOI: [10.12693/APhysPolA.131.102](https://doi.org/10.12693/APhysPolA.131.102)

PACS/topics: 81.70.Bt

1. Introduction

Electronics industry is a sector where soldering alloys are widely used. Since traditional soldering alloys contain lead, these materials entail certain risks for human health and environment. For this reason, the number of studies on alternative soldering alloys has been increasing everyday [1–8]. Alternatives to traditional Sn–Pb soldering alloy are expected to pose desired mechanical properties, be easy to procure and have low cost [9–12]. The Sn–9Zn alloy, the most preferred soldering alloy in recent years, stands out with its aspects such as having a melting temperature (198.5 °C) close to traditional Sn–37Pb alloy, low cost, good mechanical properties, and not causing any damage to human health and environment [13–17]. However, the alloy has low wettability and corrosion resistance due to easy oxidation of Zn, which is an active element [18–21]. For this reason, third and fourth alloy elements must be added to the Sn–Zn soldering alloy in order to increase use of alloy systems [22–25]. Cr is only one of these alloy elements. In a study by Fozzder et al. [26], it was reported that Al₂O₃ addition to the Sn–9Zn eutectic soldering alloy in nanoscale improved alloy microstructure and mechanical properties. In a study by Das et al. [22], it was reported that 0.5% Al addition was more effective compared to 0.5% Cu addition in terms of improving mechanical properties of the Sn–9Zn eutectic alloy. Alloy elements and reinforcement elements added to the Sn–Zn soldering alloy improve its mechanical properties. Therefore, this study aims to improve mechanical properties of the Sn–9Zn eutectic soldering alloy by adding different amounts of Cr.

2. Materials and method

In order to determine the effect of amount of Cr on mechanical properties the Zn–9Zn eutectic alloy, wt% Cr was added to the alloy in three different amounts (0.1, 0.5, and 0.9%). Tensile testing samples to be used in experimental studies were produced with the investment casting method in accordance with ASTM: B557M-10 standards. Plaster moulds were prepared for investment casting and sintered at 700 °C (3 °C/min) for 4 h. After sintering, the alloys were poured at 330 °C.

TABLE I

EDS results of Sn–9Zn eutectic alloys containing different amounts of Cr (wt%): (a) Sn–9Zn, (b) Sn–9Zn–0.1Cr, (c) Sn–9Zn–0.5Cr, and (d) Sn–9Zn–0.9Cr.

Figure	Location	Zn	Sn	Cr
1.a)	1	38.07	61.93	–
	2	0.57	99.43	–
	3	22.33	77.67	–
	4	1.29	98.71	–
1.b)	1	–	100	–
	2	52.07	47.93	–
	3	–	100	–
	4	3.25	96.75	–
1.c)	1	–	99.94	0.06
	2	1.30	98.70	–
	3	7.49	92.51	–
1.d)	1	0.58	99.42	–
	2	3.21	96.63	0.17

The melting process was carried out in an electric resistance furnace with a capacity of 1 kg using graphite melting pot, and temperatures were measured using Ni–Cr type-K insulated thermocouples with 0.23 mm wire

*corresponding author; e-mail: bekiryavuzer@gmail.com

diameter. In order to prevent segregations in compounds given in Table I, master alloying was carried out at 450 °C for 1 h and alloys were poured in ingots. Then the second melting was performed and tensile testing samples were casted. Samples were taken from produced casting parts for metallographic examination. Samples prepared with standard metallographic procedures were etched with 100 ml H₂O, 2 ml HCl, 10 g FeCl₃ for 45 s. In microstructure examinations and EDS analyses, Carl Zeiss Ultra Plus Gemini FEG brand scanning electron microscope was used. Rigaku D-MAX RINT-2200 Series brand device was used for XRD analysis to determine phases formed in microstructure. Copper Cu K_α radiation, 40 kV voltage and 45 mA current, 1°/102 s measurement speed and 10°–90° range were used in measurements. Shimadzu (HVM) microhardness device was used for hardness measurements. In hardness measurements, 50 g load was applied to the samples for 20 s. The samples were tested at 1 mm/min load rate using Shimadzu AG-IS brand tester which can be adjusted to 50 kN capacity.

3. Results and discussion

3.1. Microstructural characterization

SEM images of Sn–9Zn eutectic alloys containing different amounts (0.1–0.9%) of Cr (wt%) can be seen in Fig. 1.

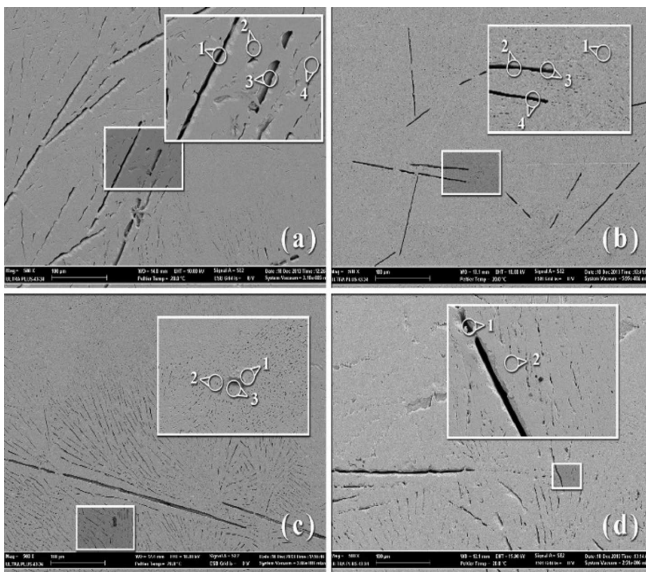


Fig. 1. SEM images of Sn–9Zn eutectic alloys containing different amounts of Cr (wt%): (a) Sn–9Zn, (b) Sn–9Zn–0.1Cr, (c) Sn–9Zn–0.5Cr, and (d) Sn–9Zn–0.9Cr.

Dark areas acicular structures and light areas are evident in microstructure SEM images of the Sn–9Zn alloy. According to EDS results given in Table I, dark areas are α -Zn-rich phases and light areas are β -Sn-rich phases, which has been mentioned in previous studies as well [3, 5, 10]. It can be seen in SEM images given

in Fig. 1 that α -Zn phases in the microstructure of the 0.1% Cr (Fig. 1b) added Sn–9Zn eutectic soldering alloy are smaller compared to the Sn–9Zn eutectic alloy (Fig. 1a). α -Zn phases in the microstructure of the 0.5% Cr (Fig. 1c) added alloy are smaller compared to 0.1% Cr added alloy. When the Cr amount is increased to 0.9% (Fig. 1d) dimensions of α -Zn phases increase and phases show an irregular distribution.

3.2. XRD results

XRD results of lead-free soldering alloys (Sn–Zn) containing different amounts of Cr (wt%) are given in Fig. 2. XRD results show that SnO₂ and Sn₂O₄ phases formed in the Sn–9Zn and Sn–9Zn–*x*Cr alloys. It can be seen from the SEM images in Fig. 1 that as the Cr ratio increases, sizes of occurring SnO and their amounts within the structure increase accordingly. Also, ZnO seem to be the common phase in all samples analysed. These results are supported by those found in the study supported by Nazeri and Mohamad [9].

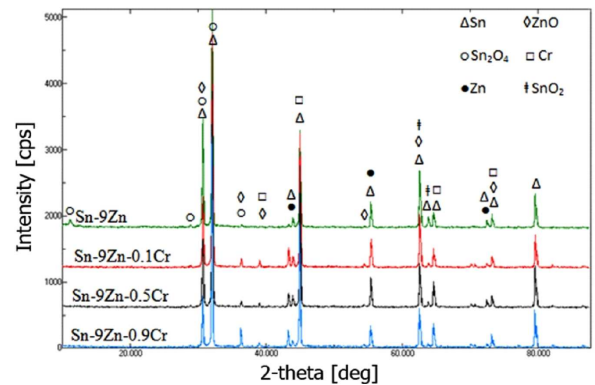


Fig. 2. XRD results of Sn–9Zn, Sn–9Zn–0.1Cr, Sn–9Zn–0.5Cr, and Sn–9Zn–0.9Cr alloys.

3.3. Tensile test and hardness results

Hardness changes in Sn–9Zn eutectic alloys containing different amounts of Cr are shown in Table II and tensile test results in Sn–9Zn eutectic alloys containing different amounts of Cr are shown in Fig. 3. Hardness test results show that the Sn–9Zn–0.1Cr alloy had the highest hardness value. An increase in the amount of Cr added to the Sn–9Zn eutectic alloy seems to result in a decrease in hardness value. However, even the alloy containing 0.9% Cr had a higher hardness value compared to the Sn–9Zn alloy. As mentioned in microstructure examinations, 0.1% Cr addition to the Sn–9Zn alloy refines Zn-rich phases and decreases the fragility of these phases. For this reason, Sn–9Zn–0.1Cr alloy has a higher hardness value than the Sn–9Zn alloy. However, 0.5% and 0.9% Cr additions cause an increase in dimensions of β -Zn-rich phases and formation of Cr-rich phases in the structure, which thus leads to a decrease in hardness. In a study by Chen et al. [23], it was noted that a Cr amount higher than 0.1% decreased alloy hardness.

TABLE II

Hardness results of Sn-9Zn, Sn-9Zn-0.1Cr, Sn-9Zn-0.5Cr, and Sn-9Zn-0.9Cr alloys

Alloy	Hardness (HV)
Sn-9Zn	16
Sn-9Zn-0.1Cr	20
Sn-9Zn-0.5Cr	19
Sn-9Zn-0.9Cr	17

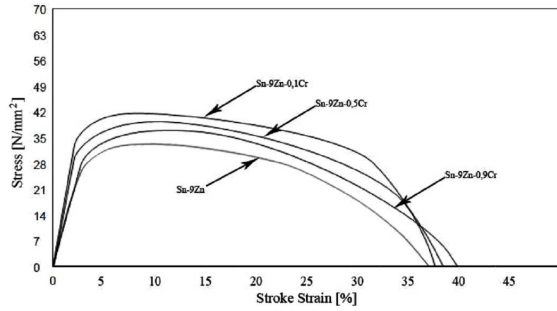


Fig. 3. Tensile test results and hardness results of Sn-9Zn, Sn-9Zn-0.1Cr, Sn-9Zn-0.5Cr, and Sn-9Zn-0.9Cr alloys.

Tensile test results show that the Sn-9Zn-0.1Cr alloy had the highest tensile strength (42 N/mm^2). The Sn-9Zn eutectic alloy, on the other hand, had the lowest tensile strength (30 N/mm^2). An increase in the amount of Cr added to the Sn-9Zn eutectic alloy seems to result in a decrease in maximum tensile strength and an increase in % elongation. 0.1% Cr addition to the Sn-9Zn alloy refines Zn-rich phases and decreases the fragility of these phases, thus the highest maximum tensile strength is obtained from this alloy. For this reason, an increase in the amount of Cr results in a decrease in tensile strength of the alloy. SEM images of fractured surfaces of alloys containing different amounts of Cr are shown in Fig. 4.

The fractured surface image of the Sn-9Zn alloy given in Fig. 4a shows that bright oxide phases formed in the structure. Fractures are believed to start from these points since these oxide phases are inconsistent with the structure. The topography of the surface shows that a ductile fracture occurred. The fractured surface SEM image of the Sn-9Zn alloy added 0.1% Cr given in Fig. 4b shows that diameters of pits in the structure increased. Greater pit diameter indicates a more ductile fracture. The fractured surface SEM image of the Sn-9Zn alloy added 0.5% Cr given in Fig. 4c shows that diameters of oxides and pits in the structure increased. These oxides are known to increase tensile strength, but decrease elongation. These elongation values were seen in tensile testing. The fractured surface SEM image of the Sn-9Zn alloy added 0.9% Cr given in Fig. 4d shows that pits became deeper and oxides grew larger. However, this alloy had the highest elongation value. When fractured surface SEM images given in Fig. 4 (a) Sn-9Zn, (b) Sn-

9Zn-0.1Cr, (c) Sn-9Zn-0.5Cr, and (d) Sn-9Zn-0.9Cr are examined, it can be seen that sizes of pits increased as the amount of chromium increased and fractures started from these oxides and pits. In addition, mostly ductile fractures occurred at these points.

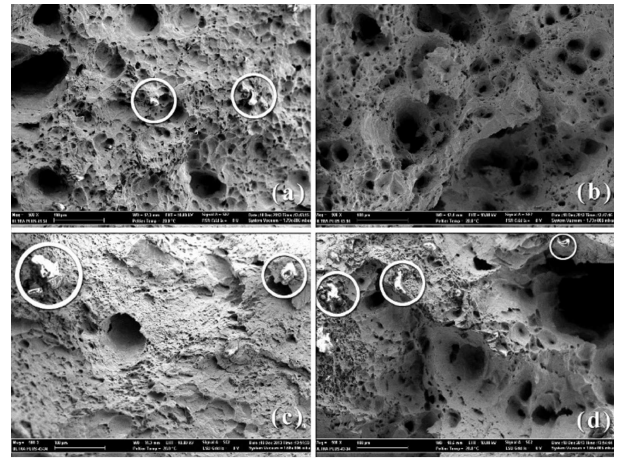


Fig. 4. SEM images of fractured surfaces of alloys containing different amounts of Cr (wt%): (a) Sn-9Zn, (b) Sn-9Zn-0.1Cr, (c) Sn-9Zn-0.5Cr, and (d) Sn-9Zn-0.9Cr.

4. Conclusion

When Cr is added to the Sn-9Zn alloy, Zn-rich phases in the microstructure become evident and a uniform structure is obtained. According to hardness results, an increase in the amount of Cr added to the Sn-9Zn eutectic alloy resulted in a decrease in hardness value. However, even the alloy containing 0.9% Cr had a higher hardness value compared to the Sn-9Zn alloy. Tensile tests show that the Sn-9Zn-0.1Cr alloy had the highest tensile strength, whereas the Sn-9Zn eutectic alloy had the lowest tensile strength. An increase in the amount of Cr added to the Sn-9Zn eutectic alloy seems to result in a decrease in tensile strength and an increase in % elongation. It was observed in fractured surface examinations that an increase in the amount of Cr resulted in an increase in oxides and pits.

References

- [1] M. Abtew, G. Selvaduray, *Mater. Sci. Eng.* **27**, 95 (2000).
- [2] L.R. Garcia, W.R. Osorio, L.C. Peixoto, A. Garcia, *Mater. Character.* **61**, 212 (2010).
- [3] R.A. Islam, Y.C. Chan, W. Jillek, S. Islam, *Microelectron. J.* **37**, 705 (2006).
- [4] R.A. Islam, B.Y. Wu, M.O. Alam, Y.C. Chan, W. Jillek, *J. Alloys Comp.* **392**, 149 (2005).
- [5] A.A. El-Daly, W.M. Desoky, A.F. Saad, N.A. Mansor, E.H. Lotfy, H.M. Abd-Elmoneim, H. Hashem, *Mater. Des.* **80**, 152 (2015).

- [6] R. Mahmudi, A. Maraghi, *Mater. Sci. Eng. A* **599**, 180 (2014).
- [7] L. Liu, P. Wu, W. Zhou, *Microelectron. Reliab.* **54**, 259 (2014).
- [8] H.R. Kotadia, P.D. Howes, S.H. Mannan, *Microelectron. Reliab.* **54**, 1253 (2014).
- [9] M.F.M. Nazeri, A. Mohamad, *Measurement* **47**, 820 (2014).
- [10] J.C. Liu, G. Zhang, J.S. Ma, K. Sukanuma, *J. Alloys Comp.* **644**, 113 (2015).
- [11] M. Liu, W. Yang, Y. Ma, C. Tang, H. Tang, Y. Zhan, *Mater. Chem. Phys.* **168**, 27 (2015).
- [12] L. Zhang, K.N. Tu, *Mater. Sci. Eng. R* **82**, 1 (2014).
- [13] C. Wang, P. Li, *Mater. Chem. Phys.* **138**, 937 (2013).
- [14] M.F.M. Nazeri, A.A. Mohamada, *J. Mater. Proc. Technol.* **219**, 164 (2015).
- [15] M.F.M. Nazeri, A.B. Ismail, A.A. Mohamad, *J. Alloys Comp.* **606**, 278 (2014).
- [16] W.R. Osorio, L.C. Peixoto, L.R. Garcia, N. Mangelick-Noel, A. Garcia, *J. Alloys Comp.* **572**, 97 (2013).
- [17] Y. Jing, G. Sheng, G. Zhao, *Mater. Des.* **52**, 92 (2013).
- [18] A.A. El-Daly, A.E. Hammad, *J. Alloys Comp.* **505**, 793 (2010).
- [19] A.A. El-Daly, A.E. Hammad, *Mater. Sci. Eng. A* **527**, 5212 (2010).
- [20] G. Ren, I.J. Wilding, M.N. Collins, *J. Alloys Comp.* **665**, 251 (2016).
- [21] M.F.M. Nazeri, A.A. Mohamad, *J. Alloys Comp.* **661**, 516 (2016).
- [22] S.K. Das, A. Sharif, Y.C. Chan, N.B. Wong, W.K.C. Yung, *J. Alloys Comp.* **481**, 167 (2009).
- [23] X. Chen, A. Hu, M. Li, D. Mao, *J. Alloys Comp.* **460**, 478 (2008).
- [24] K. Chen, S.C. Cheng, S. Wu, K.L. Lin, *J. Alloys Comp.* **416**, 98 (2006).
- [25] A.K. Gain, Y.C. Chan, A. Sharif, N.B. Wong, W.K.C. Yung, *Microelectron. Reliab.* **49**, 746 (2009).
- [26] T. Fouzder, A.K. Gain, Y.C. Chan, A. Sharif, W.K.C. Yung, *Microelectron. Reliab.* **50**, 2051 (2010).